

# INTERACTION REGION ANALYSIS FOR A HIGH-FIELD HADRON COLLIDER

Jie Wei and Stephen G. Peggs

Brookhaven National Laboratory, Upton, NY 11973, USA

Glen P. Goderre

Fermi National Accelerator Laboratory, Batavia, IL 60510, USA

1996

## ABSTRACT

The primary goal of the interaction region (IR) is to de-magnify the transverse beam dimension to a small spot size at the interaction point (IP) to reach the required luminosity. With an experimental drift space of  $\pm 25$  m and a quadrupole focusing strength of 360 T/m at the triplets, a  $\beta^*$  of 0.1 m can be achieved at a beam energy of 50 TeV. Only two families of sextupoles are needed to globally correct the chromaticity. Since the momentum spread of the beam is small ( $\sigma_p \approx 2 \times 10^{-5}$ ), a relatively large (about 20) linear chromaticity can be tolerated so that higher-order chromatic aberration produced by the low- $\beta^*$  optics is negligible. With a crossing angle of 70  $\mu$ r and a beam separation of 5  $\sigma$ , the required minimum aperture of the triplet magnets is about 3 cm. The luminosity reduction resulted from such a crossing angle is about 13%.

Crab crossing can be used to further reduce  $\beta^*$  to below 0.05 m. At the same time, luminosity degradation caused by the angle crossing is eliminated. With crab cavities positioned near the triplet operating at a voltage of a few MV, the required voltage of the 379 MHz storage rf system can be reduced from the nominal 100 MV to below 10 MV. The requirements on the accuracy of the positioning of the crab cavities and the operating voltage are both moderate. More than two families of sextupoles are needed for global chromatic compensation only when  $\beta^*$  approaches 0.05 m and below.

## I. INTRODUCTION

The design goal of a high-field hadron collider (RLHC)[1, 2, 3] is a 50 TeV storage ring that can achieve a peak luminosity of  $10^{34} \text{ cm}^{-2} \cdot \text{s}^{-1}$  with a small number of interactions per bunch-bunch collision. Table I lists the major parameters of this machine in comparison with LHC and SSC. For a round hadron beam of rms transverse beam size  $\sigma^*$  at collision, the luminosity can be expressed as

$$\mathcal{L}_0 = \frac{N_B N_0^2 f}{4\pi\sigma^{*2}}, \quad (1)$$

where  $N_B$  is the number of bunches in each ring,  $N_0$  is the number of particles in the bunch, and  $f$  is the revolution frequency. Among the quantities that determine the luminosity[3] in Eq. 1, the beam emittance reaches an equilibrium value of  $0.2\pi \text{ mm} \cdot \text{mr}$  after about 5 hours of storage due to significant synchrotron radiation (damping time  $\tau_{damp} \approx 1.2$  h). The number of particles  $N_0$  per bunch is limited by the constraints from the number of interactions per crossing, beam-beam tune shift, and instabilities. The total number of particles  $N_B N_0$  is further limited by

Table I: Comparison of major operational parameters between RLHC, LHC, and SSC at beam storage.

Quantity	Unit	SSC	LHC	RLHC
$E_s$	TeV	20	7	50
$C$	km	83	27	95
$B_0$	T	6.6	8.4	12.6
$\beta^*$	m	0.5	0.5	0.1
$\alpha$	$\mu$ r	75	200	70
$\epsilon_{N,rms}$	mm·mr	1.0	3.8	1.0
$S$	eV·s	0.73	0.63	0.22
$f_{rf}$	MHz	375	400	379
$V_{rf}$	MV	20	16	100
$\tau_{sep}$	ns	16	25	32
$\tau_{damp}$	hour	12.5	12.9	1.2
$N_0$	$10^{10}$	0.73	10.5	0.75
$N_B N_0$	$10^{14}$	1.27	2.98	0.75
$\mathcal{L}_{ini}$	$10^{34} \text{ cm}^{-2} \cdot \text{s}^{-1}$	0.1	1.0	1.1

the cryogenic constraints on radiation power. Therefore, the lattice function  $\beta^*$  at the interaction point (IP) must be small to reach the design luminosity.

The primary goal of the interaction region is to de-magnify the transverse beam dimension to a small spot size at the IP to reach the required luminosity. In Section II, we discuss various constraints that determine the practically achievable  $\beta^*$ . Field quality requirements on magnet construction and alignment are discussed in Section III. The effects of synchrotron radiation are estimated in Sections IV. Conclusions and a discussion are given in Section V.

## II. CONSTRAINTS ON IR DESIGN

The approach towards achieving an infinitesimal  $\beta^*$  is limited by various conditions. In this section, we first discuss the conditions on the crossing angle and beam separation, and then summarize the limitations imposed by the angle-crossing luminosity degradation, hourglass effect, chromatic aberrations, and triplet aperture and gradient constraints. Finally, IR parameters for the high-field collider are presented.

### A. Crossing Angle and Beam Separation

To enjoy the benefits of a relatively small bunch spacing, the beams must cross at an angle  $\alpha$  to avoid more than one bunch-bunch collision in each experimental straight section, i.e.,

$$\frac{\alpha\beta^*}{\sigma^*} = n_\alpha \gg 1, \quad (2)$$

19981026 010

I99-01-0086

where  $n_\alpha$  is usually chosen to be larger than 5. A non-zero crossing angle causes a degradation in luminosity,

$$\mathcal{L} = \mathcal{L}_0 R_\alpha, \quad R_\alpha = \left(1 + \frac{\alpha^2 \sigma_z^2}{4\sigma^{*2}}\right)^{-1/2}, \quad (3)$$

where  $\mathcal{L}_0$  is given by Eq. 1, and  $\sigma_z$  is the rms longitudinal bunch length.  $\alpha$  must also be chosen so that the condition

$$\frac{\alpha \sigma_z}{\sigma^*} \ll 1 \quad (4)$$

is satisfied.

The luminosity degradation can be eliminated by using a pair of crab[5] cavities (rf cavities operating on their transverse modes) near the IP to make the angle-crossing beams collide head-on. A brief discussion of crab crossing will be given in Section VI. Detailed studies on possible crab crossing scenarios are presented in Ref. [6].

### B. Hourglass Effect

In the experimental space near the IP, the transverse  $\beta$  function varies according to the relation

$$\beta(s) = \beta^* + \frac{s^2}{\beta^*}, \quad (5)$$

where  $s$  is the distance from the IP. When  $\beta^*$  is comparable to the longitudinal bunch dimension  $\sigma_z$ , this variation results in a reduction of luminosity (so called Hourglass effect)

$$\mathcal{L} = \mathcal{L}_0 R_H, \quad R_H = \frac{2}{\sqrt{\pi} \sigma_z} \int_0^\infty \frac{\exp(-z^2/\sigma_z^2)}{1 + z^2/\beta^{*2}} dz. \quad (6)$$

The factor  $R_H \approx 0.76$  if  $\sigma_z = \beta^*$ , and rapidly approaches unity when  $\beta^*$  is increased above  $\sigma_z$ . [4, 7] Unless novel approaches are adopted to make the focal point  $z$ -dependent (e.g., by introducing a coherent momentum spread in the bunch together with a partially uncompensated chromaticity), the condition

$$\beta^* > \sigma_z \quad (7)$$

has to be satisfied to avoid a significant luminosity degradation. The situation is unchanged with crab crossing, since crab cavities with limited voltage usually only tilt the bunch by a small amount.

### C. Chromatic Aberrations

The strong focusing produced by the IR triplet quadrupoles needed to achieve a low  $\beta^*$  inevitably generates chromatic aberrations which requires correction with sextupole families. Expressing the momentum ( $\delta \equiv \Delta p/p$ ) dependence of the transverse tunes  $\nu$  as

$$\nu = \nu_0 + \xi_0 \delta + \xi_1 \delta^2 + O(\delta^3), \quad (8)$$

the linear and second-order chromaticity produced by a low- $\beta^*$  insertion can be estimated [8, 9] as

$$\xi_0 \approx -\frac{1}{2\pi} \sqrt{\frac{\hat{\beta}}{\beta^*}}, \quad \text{and} \quad \xi_1 \approx -\frac{\hat{\beta}}{\beta^*} \cot \mu, \quad (9)$$

where the peak  $\hat{\beta}$  at the triplet is inversely proportional to  $\beta^*$  for a given machine, and  $\mu$  is the phase advance of the arc cell. When  $\beta^*$  is reduced, higher-order chromatic effects become increasingly important.

Above the transition energy, the goal of chromatic correction is to achieve a small and positive chromaticity for the entire beam, so that the machine can operate free from strong resonances and the head-tail instability. Since the dispersion is designed to be zero at the IP, and since the phase advance across the IP is  $\pi$ , the dispersion has opposite signs at the two triplets around the IP. Sextupoles for a local correction would have opposite strengths, and their non-linear kicks would act in phase, necessitating a compensation with additional sextupoles. Therefore, a global correction with multi-families of sextupoles is sometimes preferred. [9]

### D. Triplet Location and Aperture

The low- $\beta^*$  insertion quadrupoles are usually located at a certain distance from the IP for the placement of experimental detectors and solenoids. As  $\beta^*$  is reduced, the maximum  $\beta$  at the triplet increases proportionally according to Eq. 5. The aperture of the triplet quadrupoles must be large enough to provide adequate magnetic field quality. Let  $L^*$  be the free drift space between the IP and the triplet (Fig. 1),  $G$  and  $K = G/B_0\rho$  be

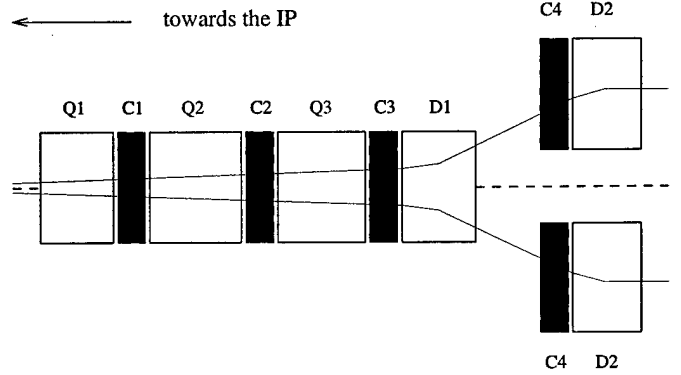


Figure 1: Schematic layout of the insertion-region magnets showing the dipoles (D1 and D2), quadrupoles (Q1, Q2, and Q3), and lumped corrector packages (C1, C2, C3, and C4) for the two counter-circulating beams.

the gradient and strength of the quadrupoles, with  $B_0$  and  $\rho$  the dipole field and machine bending radius, respectively. Then,  $\hat{\beta}$  can be approximately estimated as

$$\hat{\beta} \equiv \hat{L}^2 \beta^{*-1}. \quad (10)$$

The dependence of the effective distance  $\hat{L}$  between the triplet and the IP on the quadrupole strength  $K$  and the free drift space  $L^*$  is shown in Fig. 2. [10] Typically, the dynamic aperture of the machine is close to the “good field aperture” defined as 2/3 of the magnet coil inner diameter (ID). Supposing that common triplet quadrupoles are used to contain both beams, their minimum coil ID ( $D_{trip}$ ) can be obtained as

$$D_{trip} \approx 3 \hat{L} \left( n_{GF} \frac{\sigma^*}{\beta^*} + \frac{\alpha}{2} \right), \quad (11)$$

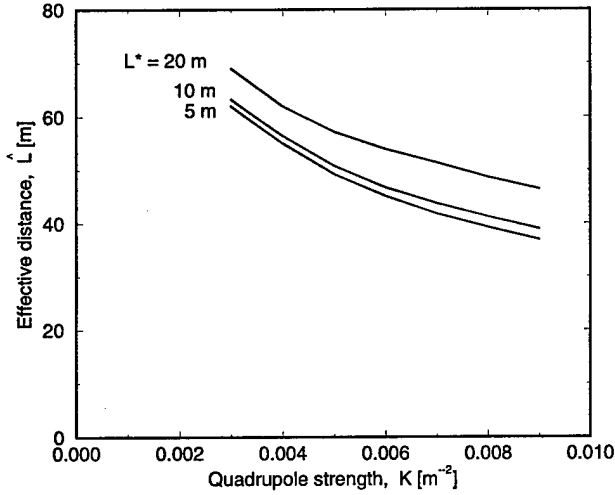


Figure 2: Effective distance  $\hat{L}$  between the IR triplets and the IP as functions of quadrupole strength  $K$  and free drift space  $L^*$ .

where the good field region contains  $n_{GF}\sigma$  of the beam, and  $n_{GF}$  is typically chosen to be 7. With such a choice, a good beam lifetime is expected for the hadron beams.

### E. Application to the High-Field Hadron Collider

For the currently proposed high-field hadron collider, two counter-circulating proton beams are stored in their separated rings of circumference 95 km at the energy of 50 TeV. With an experimental drift space of  $2L^* = 50$  m and a focusing strength of 360 T/m at the triplet, the design  $\beta^*$  is equal to 0.1 m. From Fig. 2, [10, 11] we have  $\hat{L} \approx 80$  m, and  $\beta \approx 64$  km. Assuming a  $5\sigma$  separation ( $n_\alpha = 5$ ) between the beams of an initial normalized rms emittance  $1\pi$  mm-mr, the initial crossing angle  $\alpha$  is  $70\ \mu\text{r}$ . This angle decreases from  $70\ \mu\text{r}$  to about  $30\ \mu\text{r}$  as the emittance is damped by synchrotron radiation. A minimum triplet coil ID of 32 mm provides good field region for  $7\sigma$  beams.

With the rf system operating at a peak voltage ( $V_{rf}$ ) 100 MV at frequency ( $f_{rf}$ ) 379 MHz, the rms length ( $\sigma_z$ ) of a bunch of longitudinal area ( $S$ ) 0.22 eV-s at storage is about 2 cm. The rms relative momentum deviation  $\sigma_p$  is about  $2 \times 10^{-5}$ . From Eq. 6, the hourglass effect is negligible. The luminosity degradation caused by the crossing angle is about 13% (Eq. 1).

As  $\beta^*$  reaches 0.1 m, higher-order chromatic aberration produced by the low- $\beta^*$  optics becomes noticeable. Fortunately, since the momentum spread of the beam is small, a relatively large ( $\xi_0 = 20$ ) linear chromaticity can be tolerated so that higher-order aberration is negligible in comparison. With such a choice of linear chromaticity, only two families of sextupoles are needed for a global correction. Fig. 3 shows the  $7\sigma$  tune footprints at the momentum deviation of  $\Delta p/p = -2.5\sigma_p$ , 0, and  $2.5\sigma_p$ , respectively, for the ideal lattice operating at  $\beta^* = 0.1$  m. Both horizontal and vertical linear chromaticities after sextupole compensation are 20. Since the total (head-on plus long-range) beam-beam tune shift is about 0.008, the working point is free from all resonances of order below 10.

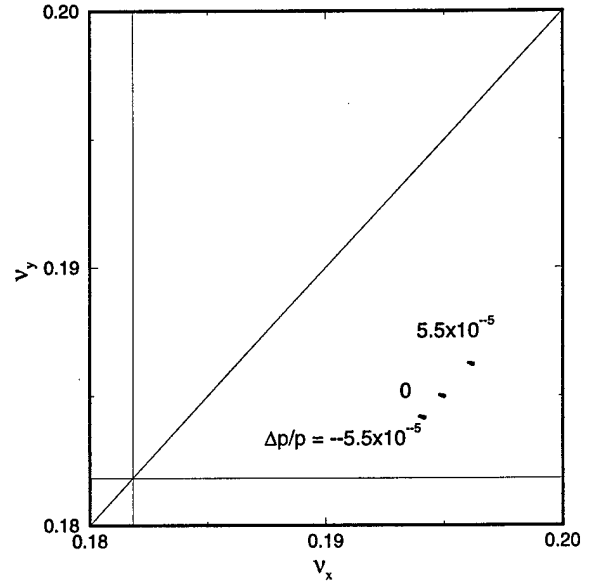


Figure 3: The tune footprint of an ideal lattice operating at  $\beta^* = 0.1$  m. Resonance lines of order 15 and below are shown.

## III. MAGNET FIELD ERROR COMPENSATION

The ultimate machine performance depends on achieving the highest possible magnetic field quality and alignment accuracy in the insertion-region triplet quadrupoles during low- $\beta^*$  operation. In this section, we first explore the sources of error during magnet construction and alignments, and then present the compensation methods.

For the following discussions, the magnet body field is expressed in terms of the multipole series  $b_n$  and  $a_n$  defined at a reference radius  $R_0$  by the relation

$$B_y + iB_x = 10^{-4} B_{ref} \left[ \sum_{n \geq 0} (b_n + ia_n) \left( \frac{x + iy}{R_0} \right)^n \right], \quad (12)$$

where  $B_{ref} = B_0$  for an arc dipole, and  $B_{ref} = GR_0$  for a quadrupole. The transverse components of the fringe field can be defined similarly in terms of the integrated value.

### A. Figure of Merit

Although the betatron phase advance is negligibly small across the triplet, the variation in transverse beam size is large from magnet body to end, and across the triplet. Therefore, error compensation of an undesired multipole  $b_n$  or  $a_n$  is based on minimizing the total action kick  $\Delta J$  in both horizontal and vertical directions across each triplet taking into account the variation of the design  $\beta$ -function [14] for both beams,

$$\frac{\Delta J_{x,y}}{J_{x,y}} \sim \frac{(2J)^{\frac{n-1}{2}}}{4\pi B_0 \rho} \frac{10^{-4} B_{ref}}{R_0^n} \int_{triplet} b_n \beta_{x,y}^{\frac{n+1}{2}} ds \quad (13)$$

and

$$\frac{\Delta J_{x,y}}{J_{x,y}} \sim \frac{(2J)^{\frac{n-1}{2}}}{4\pi B_0 \rho} \frac{10^{-4} B_{ref}}{R_0^n} \int_{triplet} a_n \beta_{x,y}^{\frac{n+1}{2}} ds, \quad (14)$$

where the integral to be minimized extends over all the quadrupole body and ends in one triplet. Typically, a multipole error is considered tolerable if  $\Delta J_{x,y}/J_{x,y}$  summed over the ring satisfies

$$\frac{\Delta J_{x,y}}{J_{x,y}} \leq 5 \times 10^{-3}. \quad (15)$$

## B. Error Sources

The leading sources of undesired harmonics are the design and construction errors in the placement of the coils at the ends and in the body of the magnets, e.g. large systematic  $b_5$  and  $a_5$  in the quadrupole lead ends, systematic  $b_5$  and random  $b_2$  in the quadrupole body.[13] The effect of the transverse fringe field contributed from the magnet ends is often significant. (On the other hand, the effect of the longitudinal fringe fields has been shown to be negligible.[12]) The secondary source is the mislocation of the iron yoke, which results in excitation dependent allowed multipoles  $b_5$  and  $b_9$  in the quadrupole body. According to Eq. 15, the tolerable systematic  $b_5$  or  $a_5$  for the 50 TeV high-field collider is about 0.5 unit at  $R_0 = 10$  mm in the absence of correction.

The separation between the closed orbits of the two beams due to the non-zero crossing angle  $\alpha$  produces a feed-down for the multipoles. The effective  $\tilde{b}_{n-1}$  produced by a multipole  $b_n$  is approximately

$$\tilde{b}_{n-1} \approx \frac{n\alpha\hat{L}}{2R_0} b_n, \quad (16)$$

where  $\hat{L}$  is defined by Eq. 10. For example, a  $b_5$  of 0.5 units for the high-field collider will produce an effective  $\tilde{b}_4$  of about 0.6 units.

The alignment procedure for the triplet assembly consists of many complicated steps. The accumulative errors from each step together with the complication caused by warm-cold transitions make it a challenging task to achieve an accurate alignment. Center offset of the quadrupoles will cause closed orbit distortion, while roll will cause transverse coupling.

## C. Compensation Methods

**Multipole optimization:** Systematic multipole errors allowed by the geometrical symmetry (e.g.,  $b_5$  and  $b_9$ ) should be minimized by iterating the coil cross section. The yoke should be designed so that its saturation helps to optimize the allowed multipoles at storage. Because of the large variation of beam transverse dimension and closed-orbit displacement from the magnet center axis, an error compensation between the fringe field and the body field of the magnet, which requires a simultaneous minimization of multipole action kick (Eq. 14) and feed-down (Eq. 16) for both beams, is difficult to achieve. A careful design is needed to eliminate errors at the magnet ends.

**Shimming:** Random errors in the magnet can be individually minimized by inserting tuning shims into the body after the magnet cold mass is constructed and measured. In the superconducting IR quadrupoles of the Relativistic Heavy Ion Collider, tuning shims are inserted into the 8 empty slots of the quadrupole body, whose variable thickness enables the individual minimization of 8 harmonics from  $a_2$  to  $a_5$  and from  $b_2$

to  $b_5$ . Recent experiments at the Brookhaven National Laboratory indicates that random errors can be reduced to about 10% of their uncorrected values.[13] Similar measures should be adopted for the construction of the superconducting IR magnets of the high-field collider.

**Choreographed welding:** During assembly of the triplet packages, the welding can be choreographed to balance distortions and to minimize offsets. The magnetic center of the quadrupoles should be accurately located relative to the external fiducials, using techniques incorporating, for example, colloidal cells or magnetic antennas, after the magnets are fully assembled in the triplet package.

**Local correctors:** Lumped correctors located in the high- $\beta$  IR region are highly effective in closed-orbit correction, local decoupling, and higher-order multipole error compensation. Fig. 1 schematically shows a possible corrector layout. Near the triplet, each beam sees a set of four corrector packages, each of 1 m length containing four corrector layers, as shown in Table II. Since the betatron phase advance is small across this

Table II: Contents of IR lumped corrector packages.

Layer	C1	C2	C3	C4
1	$a_0/b_0$	$a_1$	$b_0/a_0$	$a_0$
2	$b_2$	$a_2$	$b_2$	$a_1$
3	$b_3$	$a_3$	$b_4$	$b_2$
4	$b_5$	$a_5$	$b_5$	$b_5$

high- $\beta$  region, correction is localized. At a maximum strength of 10% of the arc dipoles (1.3 T), the two  $a_0$  correctors are capable of correcting vertical closed-orbit deviations produced by an rms quadrupole center offset of about 0.2 mm. The  $b_0$  corrector along with the independently adjustable dipole D2 are adequate to horizontally steer the beam into collision. The two  $a_1$  correctors at a strength of 10% of the IR quadrupoles (36 T/m) can be used for local decoupling to compensate an rms quadrupole roll of about 1 mr. Since the  $\beta$ -function varies rapidly, higher-order multipole corrections (e.g.,  $b_2$  and  $b_5$ ) in both horizontal and vertical directions can be best achieved with a total of four correctors for the two beams located at places with significantly different  $\beta_x/\beta_y$  ratio. The excitation strength of these higher-order correctors can be "dead-reckoned" based upon cold multipole measurements.

In addition to magnetic field errors, mechanical vibration of the triplets, often at a frequency of a few Hz, can easily cause the colliding beams to miss altogether. Feedback systems based on Beam Position Monitor measurements are necessary for a precise closed orbit control.

## IV. SYNCHROTRON RADIATION POWER

With a damping time of about two hours, synchrotron radiation plays an important role in preserving the emittance during the collider performance. The cryogenic system must be designed to absorb the radiation energy generated by the circulating particles.

In the IR triplet region, the crossing angle causes an offset of the beam closed orbit from the quadrupole center axis. The

amount of radiation energy per unit length generated by a particle is

$$U = \frac{2r_0 m_0 c^2 \gamma^4}{3\rho^2}, \quad (17)$$

where  $r_0$  is the classical radius of the particle,  $m_0 c^2$  is the rest energy, and  $\gamma$  is the relativistic factor. Compared with that in the regular arc dipole, the energy generated in the IR quadrupole can be estimated as

$$\frac{U(\text{triplet})}{U(\text{arc dipole})} \leq \left[ \frac{(\alpha + 2n_{GF}\sigma^*\beta^{*-1})\hat{L}G}{2B_0} \right]^2 \approx 0.11, \quad (18)$$

where  $G = 360$  T/m is the IR quadrupole gradient, and  $B_0 = 12.6$  T is the arc dipole field strength. The cryogenic system must be designed to absorb this power at the triplet, and measures must be taken to prevent excessive radiation background at the IP.

## V. CONCLUSIONS AND DISCUSSION

The approach towards achieving an infinitesimal  $\beta^*$  is mainly limited by the ability to correct chromatic aberration produced by the insertion region quadrupoles, and the ability to provide a short bunch length so that luminosity degradation is small (Eqs. 2, 4, and 7). With an experimental drift space of  $\pm 25$  m and a focusing strength of 360 T/m at the triplet quadrupoles, a  $\beta^*$  of 0.1 m can be achieved at the energy of 50 TeV. With the rf system operating at a peak voltage 100 MV at frequency 379 MHz, the bunch length  $\sigma_z$  is about 2 cm. The hourglass effect is therefore negligible. The crossing angle for a  $5\sigma$  beam separation is  $70\mu\text{r}$ . With such an angle, the luminosity reduction is about 13%. A minimum triplet coil ID of about 32 mm will provide a good field region for up to  $7\sigma$  beams. Only two families of sextupoles are needed to globally correct the chromaticity.

Crab crossing can be used to further reduce  $\beta^*$  to 0.05 m and below. At the same time, luminosity degradation caused by the angle crossing is eliminated. Table III compares the nominal scheme, the crabbing scheme with  $\beta^* = 0.1$  m, and with

Table III: Comparison between nominal and crabbing operations with  $\beta^* = 0.1$  m and  $\beta^* = 0.05$  m.

Quantity	Unit	Nominal	Crab I	Crab II
$\beta^*$	m	0.1	0.1	0.05
$\alpha$	$\mu\text{r}$	70	70	97
$D_{trip}$	mm	32	32	45
$V_{rf}$	MV	100	10	10
$A_B$	eV·s	34	11	11
$V_{crab}$	MV	0	3.2	4.4
$f_{crab}$	MHz	—	379	379
$\sigma_z$	mm	22	41	41
$\sigma_p$	$10^{-5}$	1.9	1.0	1.0
$R_\alpha$		0.87	1	1
$\sigma^*$	$\mu\text{m}$	1.4	1.0	1.0
$\mathcal{L}_{ini}$	$10^{34} \text{ cm}^{-2} \text{ s}^{-1}$	1.1	1.1	2.2

$\beta^* = 0.05$  m. With crab cavities positioned near the triplet operating at a voltage of 3.2~4.4 MV, the required voltage of the storage rf system can be reduced from the nominal 100 MV to about 10 MV, which still provides adequate bucket area  $A_B$  for the bunch. The requirements on the accuracy of the operating voltage and the positioning of the crab cavities are both moderate. Sextupoles of multiple families can be used to globally compensate the chromatic aberration.

To achieve an even lower  $\beta^*$ , the bunch length needs to be reduced accordingly to avoid the hourglass effect. For example with  $\beta^* = 0.025$  m, with crab crossing and a higher rf frequency of 758 MHz, the required rf voltage is about 100 MV. The ultimate challenge, however, is to achieve satisfactory chromatic compensation.

## VI. ACKNOWLEDGMENTS

The authors would like to thank G. Dugan, M. Harrison, M. Syphers, and S. Tepikian for many helpful discussions.

## VII. REFERENCES

- [1] *Proceedings of the Workshop on Future Hadron Facilities in the US*, Bloomington, FERMILAB-TM-1907, 1994.
- [2] *Beyond the LHC: A Conceptual Approach to a Future High Energy Hadron Collider*, M. J. Syphers, M. A. Harrison, S. Peggs, Dallas, PAC Proc., 1995, p. 431.
- [3] *Really Large Hadron Colliders*, G. Dugan, Invited talk at 1996 DPF/DPB Summer Study on New Directions for High-Energy Physics, Snowmass, 1996.
- [4] *Beam-Beam Instability*, A. Chao, AIP Conf. Proc. 127, *Physics of High Energy Particle Accelerators*, ed. M. Month, P.F. Dahl, M. Dienes, 1983, p. 202.
- [5] *Energy Scaling, Crab Crossing and the Pair Problem*, R. B. Palmer, Invited talk at the DPF Summer Study Snowmass 88, SLAC-PUB-4707, Stanford 1988.
- [6] *Crab Crossing in a Large Hadron Collider*, J. Wei, these proceedings, 1996.
- [7] *Review of Linear Collider Beam-Beam Interaction*, P. Chen, AIP Conf. Proc. 184, *Physics of High Energy Particle Accelerators*, ed. M. Month, M. Dienes, 1989, p. 634.
- [8] *Elementary Design and Scaling Considerations of Storage Ring Colliders*, A. Chao, AIP Conf. Proc. 153, *Physics of High Energy Particle Accelerators*, ed. M. Month, M. Dienes, 1987, p. 104.
- [9] *Chromaticity*, A. Verdier, CERN Fourth Advanced Accelerator Physics Course, ed. S. Turner, 1992, p. 204.
- [10] *Minimising Chromaticity in Interaction Regions with Long Weak Quadrupoles*, S. Peck, Proc. SSC Summer Study, Snowmass, 1984, p. 384.
- [11] *Lattices for a High-Field 30 TeV Hadron Collider*, S. Peggs, et. al., these proceedings, (1996).
- [12] *Theorem on Magnet Fringe Field*, J. Wei, R. Talman, Particle Accelerators, **55**, 339 (1996).
- [13] *Large Aperture Quadrupoles for RHIC Interaction Region*, R. Gupta, et. al., Proc. 1993 Part. Accel. Conf., Washington, D.C., 1993, p. 2745.
- [14] *Error Compensation in Insertion-Region Magnets*, J. Wei, Particle Accelerators, **55**, 439 (1996).

**INTERNET DOCUMENT INFORMATION FORM**

**A . Report Title:** Interaction Region Analysis for A High-Field  
Hadron Collider

**B. DATE Report Downloaded From the Internet** 10/19/98

**C. Report's Point of Contact: (Name, Organization, Address,  
Office Symbol, & Ph #):** Brookhaven National Laboratory  
Upton, NY 11973

**D. Currently Applicable Classification Level:** Unclassified

**E. Distribution Statement A:** Approved for Public Release

**F. The foregoing information was compiled and provided by:**  
**DTIC-OCA, Initials:** VM\_ **Preparation Date:** 10/20/98\_\_

The foregoing information should exactly correspond to the Title, Report Number, and the Date on the accompanying report document. If there are mismatches, or other questions, contact the above OCA Representative for resolution.